

Received: 2021.10.03  
Accepted: 2021.11.25  
Available online: 2021.12.14  
Published: 2021.12.24

# Lotus Seedpod Proanthocyanidins Protect Against Light-Induced Retinal Damage via Antioxidative Stress, Anti-Apoptosis, and Neuroprotective Effects

Authors' Contribution:  
Study Design A  
Data Collection B  
Statistical Analysis C  
Data Interpretation D  
Manuscript Preparation E  
Literature Search F  
Funds Collection G

ABG 1 **Jianmei Wang**   
B 2 **Tao Yu**  
C 1 **Liuqing Sheng**   
D 3 **Hui Zhang**  
A 1 **Fei Chen**  
F 1 **Jie Zhu**  
AE 4 **Mingxing Ding**

1 College of Pharmaceutics, Jinhua Polytechnic, Jinhua, Zhejiang, PR China  
2 Pharmacy Department, Jinhua Wenrong Hospital, Jinhua, Zhejiang, PR China  
3 Jinhua Center of Laboratory Animals, Jinhua Municipal Food and Drug Inspection Institute, Jinhua, Zhejiang, PR China  
4 Medical Molecular Biology Laboratory, School of Medicine, Jinhua Polytechnic, Jinhua, Zhejiang, PR China

**Corresponding Authors:** Jianmei Wang, e-mail: 20101014@jhc.edu.cn, Mingxing Ding, e-mail: mtd5tc@163.com  
**Financial support:** This work was funded by the Science and Technology Project of Jinhua City in China (2020-4-093)  
**Conflict of interest:** None declared

**Background:** Over-exposure to visible white light can cause retinal damage. Lotus seedpod proanthocyanidins (LSPCs) possess a variety of biological activities, including potent antioxidant and protective effects. Herein, this study observed whether LSPCs can protect against light exposure-induced retinal damage.

**Material/Methods:** We randomly separated 40 Prague-Dawley rats into a control group, a light exposure-induced retinal injury model group, and low-dose (50 mg/kg), medium-dose (100 mg/kg), and high-dose (100 mg/kg) LSPCs groups. Light-induced retinal damage models were established by 5000±200 Lx light treatment for 6 h. Five days and 0.5 h before the light treatment, rats in the LSPCs groups were separately administered 50, 100, and 200 mg/kg LSPCs by gavage. After 7 days, H&E staining of retinal sections was performed and the thickness of the ONL was measured. Oxidative stress-related markers and antioxidant enzymes were measured in serum by biochemical testing. TUNEL staining of retinal sections was also performed. Apoptosis-relevant proteins were examined by RT-qPCR and western blotting. GFAP expression was examined with immunohistochemistry.





**Results:** Our H&E staining showed that LSPCs can prevent retinal degeneration following light exposure. Histological analysis showed a significant reduction in the ONL thickness of light exposure-induced retinal injury rats, but LSPCs substantially improved the ONL thickness. LSPCs markedly ameliorated the light-induced increase in levels of MDA, NO, and NOS, and decrease in activity of GSH-Px and SOD. Moreover, LSPCs treatment alleviated light-induced retinal apoptosis and limited the light-induced increase in GFAP expression.

**Conclusions:** LSPCs effectively attenuated light-induced retinal damage through antioxidative stress, anti-apoptosis, and neuroprotective effects.

**Keywords:** **Apoptosis • Neuroprotection • Oxidative Stress • Proanthocyanidins**

**Abbreviations:** **LSPCs** – lotus seedpod proanthocyanidins; **H&E** – Hematoxylin and Eosin; **ONL** – outer nuclear layer; **MDA** – malondialdehyde; **NO** – nitric oxide; **NOS** – nitric oxide synthase; **GSH-Px** – glutathione peroxidase; **SOD** – superoxide dismutase; **TUNEL** – Terminal-deoxynucleotidyl Transferase-Mediated Nick-End Labeling; **RT-qPCR** – real-time quantitative polymerase-chain reaction; **HRP** – horseradish peroxidase; **IHC** – immunohistochemistry; **GFAP** – glial fibrillary acidic protein

**Full-text PDF:** <https://www.medscimonit.com/abstract/index/idArt/935000>

 3427  1  8  33



## Background

Light is the basic element needed for vision and modulating circadian rhythms, but excessive light has negative effects on the survival of a variety of types of retinal cells [1]. Increasing evidence suggests that excessive visible white light exposure can cause human retinal damage, which is the major cause of age-related macular degeneration (AMD) occlusion and progression [2]. Unfortunately, there are no effective drugs against AMD and preventive drugs are needed. Thus, it is of importance to develop effective drugs against light-induced retinal damage.

Proanthocyanidins are natural polyphenols widely found in common foods such as cereals, fruits, vegetables, and wines [3,4]. **Figure 1** depicts the chemical formula of proanthocyanidins. They possess excellent antioxidant activity and multiple biological activities, which have been applied in food, cosmetics, and medicine [5-7]. The lotus seedpod is an inedible part of the plant *Nelumbo nucifera* Gaertn [8]. Lotus seedpod is another important source of proanthocyanidins, as is grape seed [9]. Lotus seedpod proanthocyanidins (LSPCs) have been successfully extracted and characterized as a variety of molecules, including catechin/epicatechin monomers, dimers, trimers, and tetramers, as well as quercetin glucuronide [10]. Among these, catechin and epicatechin are the basic units, while dimers are the main ingredient [11]. LSPCs display potent antioxidant ability as well as strong protective effects on human health [12]. For instance, LSPCs can effectively protect against methyl-mercuric chloride damage-induced neurotoxicity through improving the antioxidant defense ability by modulating the Nrf2/HO-1 pathway, and can also inhibit the mitochondrial-mediated apoptosis pathway [12]. LSPCs can ameliorate d-galactose-induced cognitive impairment and brain aging in senescent mice, suggesting the therapeutic role of LSPCs in treating Alzheimer disease [13]. LSPCs ameliorate learning and memory damage in mice with amnesia induced by scopolamine [14]. LSPC can

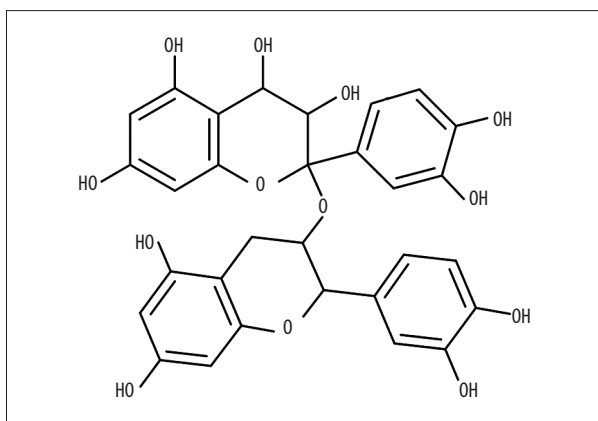


**Figure 1.** The chemical formula of proanthocyanidins. PowerPoint (version 2020; Microsoft, USA) was used to create the picture.

modulate the NO/ADMA/DDAH pathway through suppressing oxidative stress to alleviate insomnia in rats [15].

Although previous research has suggested a variety of pharmacological activities LSPCs, the protective effects of LSPCs on light-induced retinal damage are still unclear. Hence, this study observed the cytoprotective mechanisms of LSPCs against LSPCs on light exposure-induced retinal injury in rats. Our findings could expand the medicinal use of lotus root, while LSPCs have potential to preventive light-induced retinal damage.

## Material and Methods

### Animals

Forty clean-grade Sprague-Dawley rats (20 males and 20 females) were obtained from the Jinhua Laboratory Animal Center (Zhejiang, China). The age of the rats was 6-8 weeks and the weight was  $180 \pm 20$  g. The rats were adapted for 1 week in an alternating light-dark environment at  $22 \pm 2^\circ\text{C}$ , and  $55 \pm 10\%$  humidity. All rats were allowed to move freely.

### Construction of a Light-Induced Retinal Damage Model

LSPCs (purity >98%) were isolated from lotus seedpods. All rats were randomly divided into a control group, a light-induced retinal damage model group, a low-dose LSPCs group, a medium-dose LSPCs group, or a high-dose LSPCs group, with 8 rats in each group. Five days before the light treatment, rats in the low-dose LSPCs group, medium-dose LSPCs group, and high-dose LSPCs group were separately administered 50 mg/kg LSPCs, 100 mg/kg LSPCs, or 200 mg/kg LSPCs by gavage. Meanwhile, rats in the light-induced retinal damage model group and control group were given an equal volume of 0.9% normal saline by gavage. At 0.5 h before light treatment, administration by gavage was performed in each group again. Rats in the light-induced retinal damage model group, low-dose LSPCs group, medium-dose LSPCs group, and high-dose LSPCs group were subjected to  $5000 \pm 200$  Lx light treatment in a custom-designed light box for 6 h. After the illumination was completed, the treated rats were returned to the original light-dark cycle lighting environment and kept for 1 week. On the 7<sup>th</sup> day after light treatment, the rats were anesthetized and blood was taken from the orbital venous plexus. Finally, the rat was euthanized and the eyeballs were taken out. All the experimental procedures were performed in line with the protocols approved by the Institutional Animal Care and Use Committee of Jinhua Polytechnic (2019020).

### Hematoxylin & Eosin (H&E) Staining

Eyeball tissue was fixed by 4% paraformaldehyde (Servicebio, Wuhan, China) for 12 h. Part of the cornea was taken out and

fixed again for 8 h. After dehydration and paraffin embedding, the tissue was sectioned into 5- $\mu$ M slices. After that, H&E staining of retina tissues was carried out. The sections were stained by hematoxylin (#B600020; Proteintech, Wuhan, China) for 5 min. Afterwards, the section was rinsed with alkaline PBS for 2 min to return to the blue. After being rinsed under running water for 3 min, the sections were stained by eosin (Sigma, USA) for 10 min at room temperature. The sections were then quickly washed with distilled water, followed by 70%, 80%, and 90% ethanol. Then, the sections were treated with 95% ethanol for 30 s and 100% ethanol for 3 min, twice each, and then treated twice by xylene (#10023418; China National Pharmaceutical Group Corporation) for 5 min. Neutral gum was used to mount the film. Images were acquired under a BX53 microscope (Olympus, Japan). The thickness of the outer nuclear layer (ONL) distant from optic nerve head was calculated.

### Biochemical Testing

The blood from orbital venous plexus was ultracentrifuged at 4°C and the supernatant was harvested. Kits of malondialdehyde (MDA; #A005-1), nitric oxide (NO; #A013-2), nitric oxide synthase (NOS; #A014-2), glutathione peroxidase (GSH-Px; #A014-2), and superoxide dismutase (SOD; #A001-3) were purchased from Nanjing Jiancheng Bioengineering Institute (China). According to the manufacturer's instructions, the activity or level of MDA, NO, NOS, GSH-Px, and SOD was determined with an enzyme-linked immunosorbent assay (ELISA) spectrophotometry reader.

### Terminal-Deoxynucleotidyl Transferase-Mediated Nick-End Labeling (TUNEL)

The TUNEL Apoptosis Detection Kit (FITC; #ATK00001) was purchased from Atagenix Company. The paraffin tissue sections were deparaffinized in xylene for 20 min at room temperature. Fresh xylene and dewax were changed for another 20 min. Then, the sections were soaked by gradient ethanol (100%, 95%, 80%, and 70%) at room temperature. The sections were rinsed with PBS for 5 min as well as permeabilized by 0.02  $\mu$ g/ $\mu$ l Proteinase K solution for 15-20 min. Then, the sections were washed with PBS 3 times (5 min each time). The positive control group was treated with 10 U/ml DNase I, while the negative control group was treated with an equal volume of 1 $\times$  DNase I Buffer. Each group was also treated with 1 $\times$  DNase I Buffer and incubated for 10 min. Then, excess liquid was removed and the slide was washed by deionized water. TUNEL solution was prepared, including the following ingredients: 1 $\times$  equilibration buffer, fluorescein-12-dUTP nucleotide, recombinant TdT enzyme, and ddH<sub>2</sub>O. The sections were treated by TUNEL reagent in the dark for 60 min and immersed in PBS solution twice at 37°C. After absorbing the excess water on the sections, 0.05  $\mu$ g/ $\mu$ l DAPI (#D9542; Sigma, USA) was added

**Table 1.** Primer sequences for RT-qPCR.

| Primer                      | Sequence (5'-3')      |
|-----------------------------|-----------------------|
| Rat- $\beta$ -actin-forward | CTGTGTGGATTGGTGGCTCT  |
| Rat- $\beta$ -actin-reverse | CAGCTCAGTAACAGTCCGCC  |
| Rat-Caspase-3-forward       | TTGGAACGGTACGCCGAAGAA |
| Rat-Caspase-3-reverse       | ACACAAGCCATTTCAGGGT   |
| Rat-p53-forward             | GCGTTGCTCTGATGGTG     |
| Rat-p53-reverse             | CCGAAAAGTCTGCCTGTC    |
| Rat-Bcl-2-forward           | CTGGTGGACAACATCGCTCT  |
| Rat-Bcl-2-reverse           | GCATGCTGGGGCCATATAGT  |
| Rat-Bax-forward             | GGGCCTTTTGTACAGGGT    |
| Rat-Bax-reverse             | TTCTTGGTGGATGCGTCTCG  |

dropwise to the sections. After immersion, anti-fluorescence quenching munter was used to mount the sections. Images were acquired under an UltraVIEW VoX & IX81 fluorescence microscope (Olympus). The excitation wavelength range was 450-500 nm, and the emission wavelength range was 515-565 nm.

### Real-Time Quantitative Polymerase-Chain Reaction (RT-qPCR)

Total RNA was extracted from eyeball tissues via Trizol reagent (#9109; TaKaRa, Dalian, China), which was quantified by Nanodrop2000 spectrophotometer (Thermo Fisher, USA). Extracted RNA was reverse transcribed to synthesize cDNA with an iScript cDNA Synthesis Kit (#1708890; Bio-Rad, USA) under the following 20- $\mu$ L reverse transcription system: 4  $\mu$ L  $\times$  iScript Reaction Mix, 1  $\mu$ L iScript Reverse Transcriptase, and 1  $\mu$ g RNA template and nuclease-free water. On the CFX Connect fluorescence quantitative PCR instrument (Bio-Rad, USA), RT-qPCR was then presented under the following 10- $\mu$ L reaction system: 5  $\mu$ L iTaq™ universal SYBR Green supermix (2 $\times$ ), 1  $\mu$ L forward and reverse primers, 2  $\mu$ L DNA template, and 2  $\mu$ L H<sub>2</sub>O. The reaction procedure was as follows: at 95°C for 5 min, 40 cycles of 95°C for 10 s, and 60°C for 30 s. The melting curve temperature was 65°C to 95°C. **Table 1** lists the primer sequences of Caspase-3, p53, Bcl-2, and Bax. The mRNA expression of the above genes was determined using the 2<sup>- $\Delta\Delta$ CT</sup> method with  $\beta$ -actin as a reference.

### Western Blotting

Eyeball tissues were ground to powder in a mortar with addition of liquid nitrogen. The tissues were lysed using RIPA lysate (Beyotime, China) on ice for 0.5 h and transferred to an EP tube. Then, the samples were ultrasonicated for 3 min and centrifuged at 12 000 g at 4°C for 20 min. The supernatant samples were then moved in another EP tube. Using BCA kits (Beyotime), the protein concentrations were quantified. The

samples were added to 5×SDS loading buffer (#S8010; Solarbio, China) and boiled at 100°C for 5 min. Afterwards, the sample was separated via 8% SDS-PAGE and transferred onto PVDF membranes for 1.5 h. The membrane was sealed by 5% milk/TBST for 1 h. Primary antibody was diluted with 1% BSA/PBST according to the recommended dilution ratio. The membrane was incubated by primary antibody against cleaved Caspase-3 (1: 1000; #9664T; CST, USA), Caspase-3 (1: 1000; #9662S; CST), p53 (1: 1000; #60283-2-Ig; Proteintech, Wuhan, China), Bcl-2 (1: 1000; #26593-1-AP; Proteintech) and Bax (1: 1000; #60267-1-AP; Proteintech) at 4°C overnight and incubated with horseradish peroxidase (HRP)-labeled goat anti-rabbit secondary antibody (1: 5000; #SA00001-2; Proteintech) at room temperature for 1 h. The protein bands were developed and analyzed using the ChemiDoc™XRS+ Gel imaging system (Bio-Rad, USA).

### Immunohistochemistry (IHC)

IHC kits (#KIHC-5) were purchased from Proteintech, Inc. The paraffin-embedded sections were deparaffinized and hydrated, then incubated with 3% hydrogen peroxide for 10 min at room temperature. After antigen retrieval, the sections were blocked with goat serum (#C0265; Beyotime) for 20 min. The sections were incubated with primary antibody against glial fibrillary acidic protein (GFAP; 1: 100; #ab7260; Abcam, USA) at 37°C for 90 min. The sections were incubated with HRP-labeled secondary antibody (1: 200; #SA00001-2; Proteintech) for 30 min at 37°C. The sections were developed and reacted with a color developing agent (DAB) for 10 min. The degree of color was assessed under an IX71 microscope (Olympus, Japan). The color reaction was terminated by addition of distilled water. Nuclei were counterstained by hematoxylin (#B600020; Proteintech) for 5 min, and rinsed with running water for blueing. After dehydration, the sections were sealed with neutral gum.

### Statistical Analysis

All analyses were performed using GraphPad Prism software (version 8.0.1; Graph Pad; San Diego, CA, USA). Eight rats were set in each group, which were adequate and representative. Data are expressed as mean±standard deviation. Statistical analyses were conducted with one-way analysis of variance (ANOVA) or Turkey's post hoc test.  $P<0.05$  was set as the criterion for statistical significance.

## Results

### LSPCs Preserve Retinal Degeneration Following Light Exposure

To investigate the efficacy of LSPCs treatment in preventing light-induced retinal damage, histological analyses were carried

out using H&E staining. **Figure 2** shows the structure of retina of the rats from the control group was complete, the nerve fibers were arranged neatly, and the ganglion cell gap was clear. The retinal nerve fibers of the light exposure-induced retinal injury rats were not arranged neatly, the interstitium had edema, the cell layer was vacuolated, and the number of retinal ganglion cells was significantly reduced. The optic nerve fibers of the rats in the low-dose and medium-dose LSPCs groups were irregularly arranged, the fibrous interstitium was partially edematous, and occasionally vacuoles were found. The structure of retina of the rats in the high-dose LSPCs group was complete and the cells were arranged neatly. These findings suggest the protective effects of LSPCs retinal morphology following light exposure.

### LSPCs Preserve Retinal Morphology in Light-Induced Retinal Damage Rats

The ONL thickness was measured at 1920, 1680, 1440, 1200, 960, 720, 480, and 240 μm superior and inferior to the optic nerve head according to H&E staining of retinal sections. Compared with the control group, a pronounced reduction in the thickness of ONL was found in the light-induced retinal damage model group (**Figure 3A, 3B**). In contrast, low-, medium-, and high-dose LSPCs prominently increased the thickness of ONL of light-induced retinal damage model rats in a dose-independent manner (**Figure 3A, 3B**). Hence, our findings indicate the protective effects of LSPCs retinal morphology following light exposure.

### LSPCs Exert an Antioxidative Effect On Light-Induced Retinal Damage

Biomarkers of oxidative stress – MDA, NO, and NOS – were measured in serum of rats in all groups. Compared with the control group, we observed a substantial increase in serum MDA, NO, and NOS levels in the light-induced retinal damage model group (**Figure 4**). Low-dose LSPCs did not alter serum MDA levels but distinctly decreased serum NO and NOS levels in the light-induced retinal damage model rats. Moreover, medium- and high-dose LSPCs substantially decreased serum MDA, NO, and NOS levels in the light-induced retinal damage model rats. Two antioxidant enzymes – GSH-Px and SOD – were also tested in serum samples. A substantial decrease in serum GSH-Px and SOD activity was seen in the light exposure-induced retinal injury model group in comparison to the control group (**Figure 4**). Low-dose LSPCs did not affect GSH-Px or SOD activity in the serum of light-induced retinal damage model rats. However, serum GSH-Px and SOD activity was distinctly increased by medium- and high-dose LSPCs in light-induced retinal damage model rats. Thus, the results of this study show an antioxidative effect of LSPCs on light-induced retinal damage.



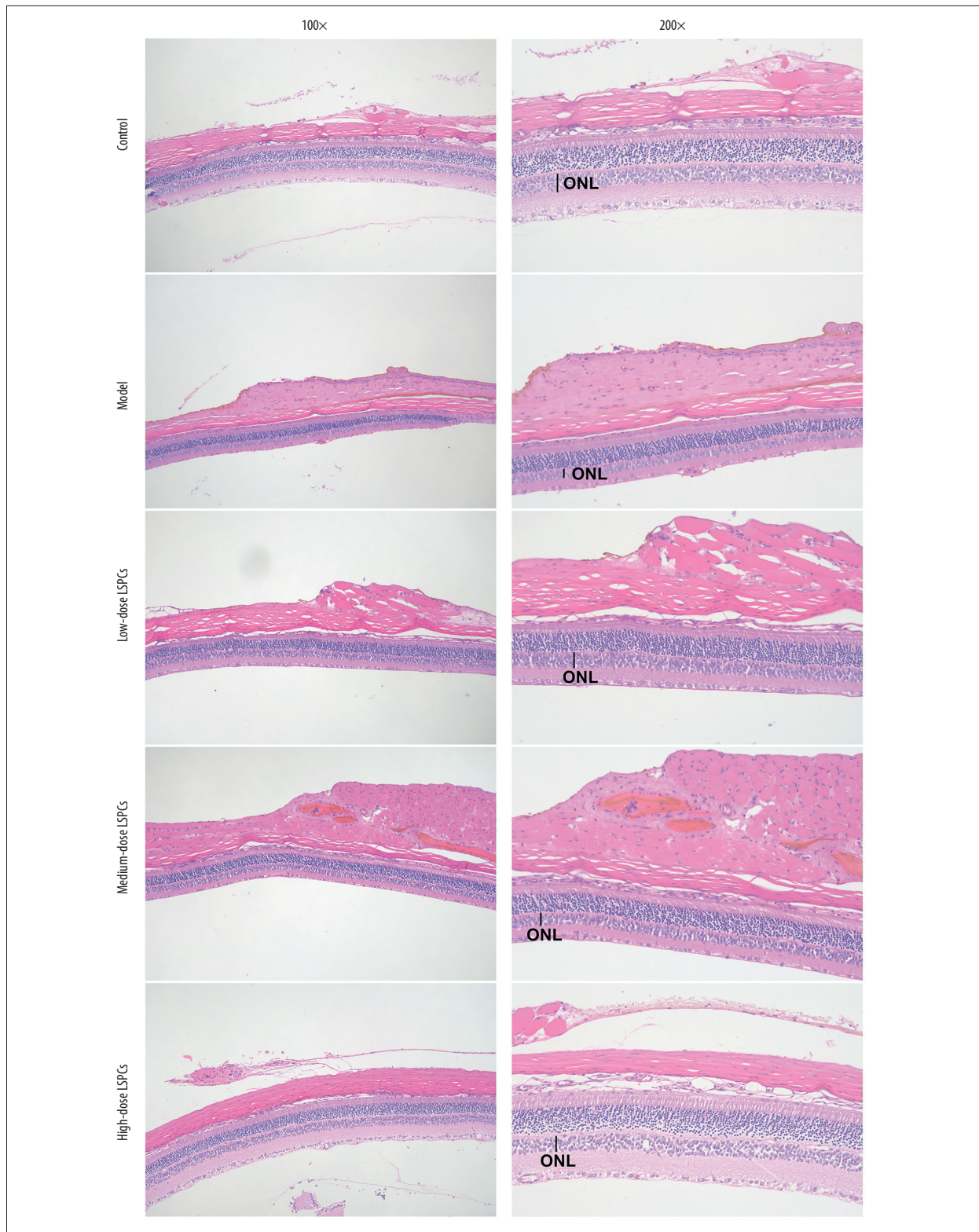


**Figure 2.** Protective roles of LSPCs on retinal structure in light-induced retinal damage rats. Histological analysis was carried out utilizing H&E staining. Representative images of H&E staining of control, light exposure-induced retinal injury model, low-, medium-, and high-dose LSPCs groups were shown, separately. Magnification, 100× or 200× bar value, 50 or 100 μm. Olympus software (version 2.2; Olympus, Japan) was used to create the pictures.

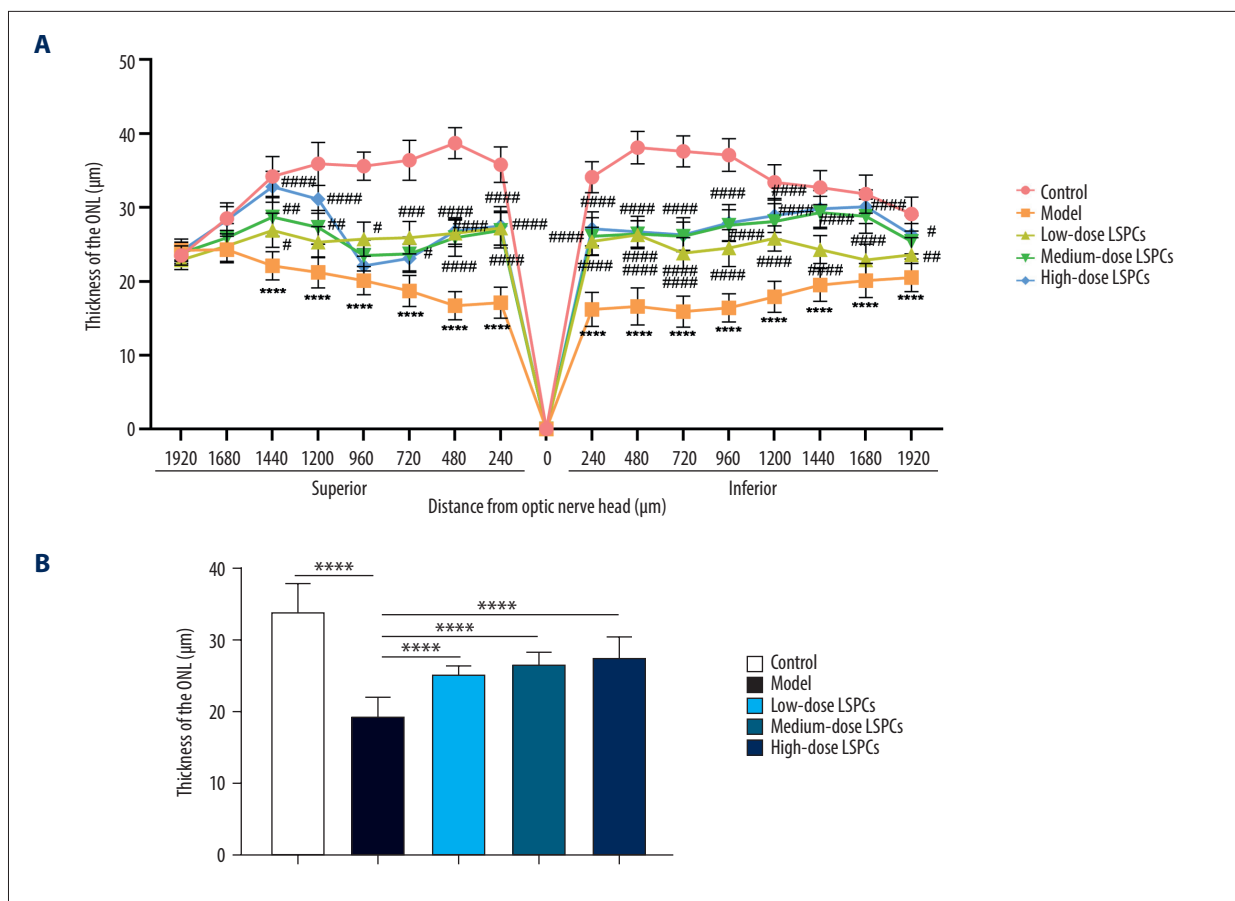


**Figure 3.** LSPCs improved retinal morphology of light exposure-induced retinal injury rats. **(A)** The thickness values of outer nuclear layer (ONL) were measured at 1920, 1680, 1440, 1200, 960, 720, 480, and 240  $\mu\text{m}$  superior and inferior to the optic nerve head in control, light-induced retinal damage model, low-, medium-, and high-dose LSPCs groups. Compared with the control group, \*\*\*\*  $P < 0.0001$ ; compared with model group, #  $P < 0.05$ ; ##  $P < 0.01$ ; ###  $P < 0.001$ ; ####  $P < 0.0001$ . **(B)** The mean of thickness value of ONL was calculated in each group. \*\*\*\*  $P < 0.0001$ . GraphPad Prism software (version 8.0.1; Graph Pad; San Diego, CA, USA) was used to create the pictures.

### LSPCs Alleviate Retinal Apoptosis Following Light Exposure

TUNEL staining of retinal sections was used for assessing cell apoptosis in retinal tissues. Compared with the control group, a significant increase in retinal apoptosis was found in the light exposure-induced retinal injury model rats (Figure 5). In contrast, low-, medium-, and high-dose LSPCs substantially reduced light-induced retinal apoptosis. Apoptotic and pro-apoptotic biomarkers were measured with RT-qPCR. We observed a marked increase in the mRNA expression of apoptotic Caspase-3, p53, and Bax in the light exposure-induced retinal injury model rats compared with the control group (Figure 6A-6C). Low-, medium-, and high-dose LSPCs markedly reduced the mRNA expression of Caspase-3 and Bax in retinal tissues with light-induced damage. However, low- and medium-dose LSPCs did not alter the light exposure-induced increase in mRNA expression of p53 in retinal tissues. A substantial reduction in the mRNA expression of p53 was induced by high-dose LSPCs in retinal

tissues with light-induced damage. Moreover, compared with the control group, we observed a significant decrease in the mRNA expression of pro-apoptotic Bcl-2 in the light-induced retinal damage model group (Figure 6D). Low-dose LSPCs did not affect the mRNA expression of pro-apoptotic Bcl-2 in light exposure-induced retinal tissues. In contrast, the mRNA expression of pro-apoptotic Bcl-2 was markedly elevated by medium- and high-dose LSPCs in the light exposure-induced retinal injury model rats. This research also measured the expression of apoptotic and pro-apoptotic biomarkers with western blotting. Our results demonstrated that the expressions of pro-Caspase-3, cleaved Caspase-3, p53, and Bax proteins were markedly higher in the light exposure-induced retinal injury model rats in comparison to the control group (Figure 7A, 7B). Nevertheless, low-, medium-, and high-dose LSPCs all substantially reduced the expressions of pro-Caspase-3, cleaved Caspase-3, p53, and Bax proteins in light exposure-induced retinal tissues, in a dose-independent manner. The pro-apoptotic

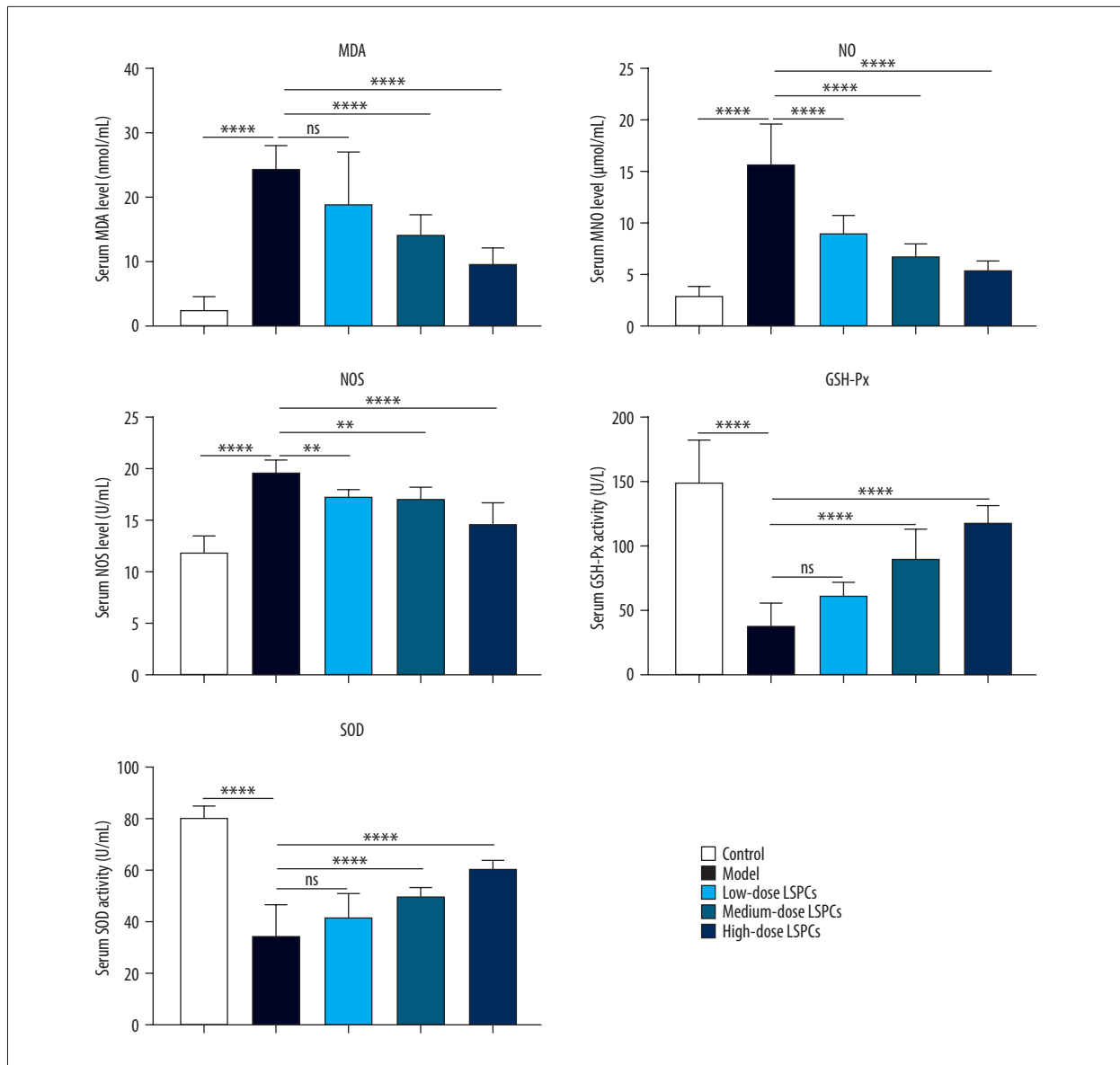


**Figure 4.** Treatment of LSPCs decreased oxidative stress in light-induced retinal damage rats. Serum MDA and NO levels as well as serum NOS, GSH-Px, and SOD activities were quantified in control, light-induced retinal damage model, low-, medium-, and high-dose LSPCs groups. Ns – not significant; \*\*  $P < 0.01$ ; \*\*\*  $P < 0.001$ ; \*\*\*\*  $P < 0.0001$ . GraphPad Prism software (version 8.0.1; Graph Pad; San Diego, CA, USA) was used to create the pictures.

protein Bcl-2 and Bcl-2/Bax ratio were also measured. We observed a marked reduction in Bcl-2 expression and Bcl-2/Bax ratio in the light exposure-induced retinal damage models in comparison to controls (Figure 7A, 7B). In contrast, low-, medium-, and high-dose LSPCs markedly increased Bcl-2 expression and Bcl-2/Bax ratio in light exposure-induced retinal tissues. Collectively, LSPCs alleviated retinal apoptosis following light exposure.

### LSPCs Has Neuroprotective Effects On Light-Induced Retinal Damage

Müller glia cell reactive gliosis, which can have a neuroprotective effect in the early stage following injury, was evaluated through IHC staining for GFAP, a marker for reactive Müller cells and astrocytes. Compared with the control group, GFAP expression was substantially increased in the light exposure-induced retinal damage model group (Figure 8). Following treatment with LSPCs, GFAP expression was markedly reduced in the light exposure-induced retinal damage models.

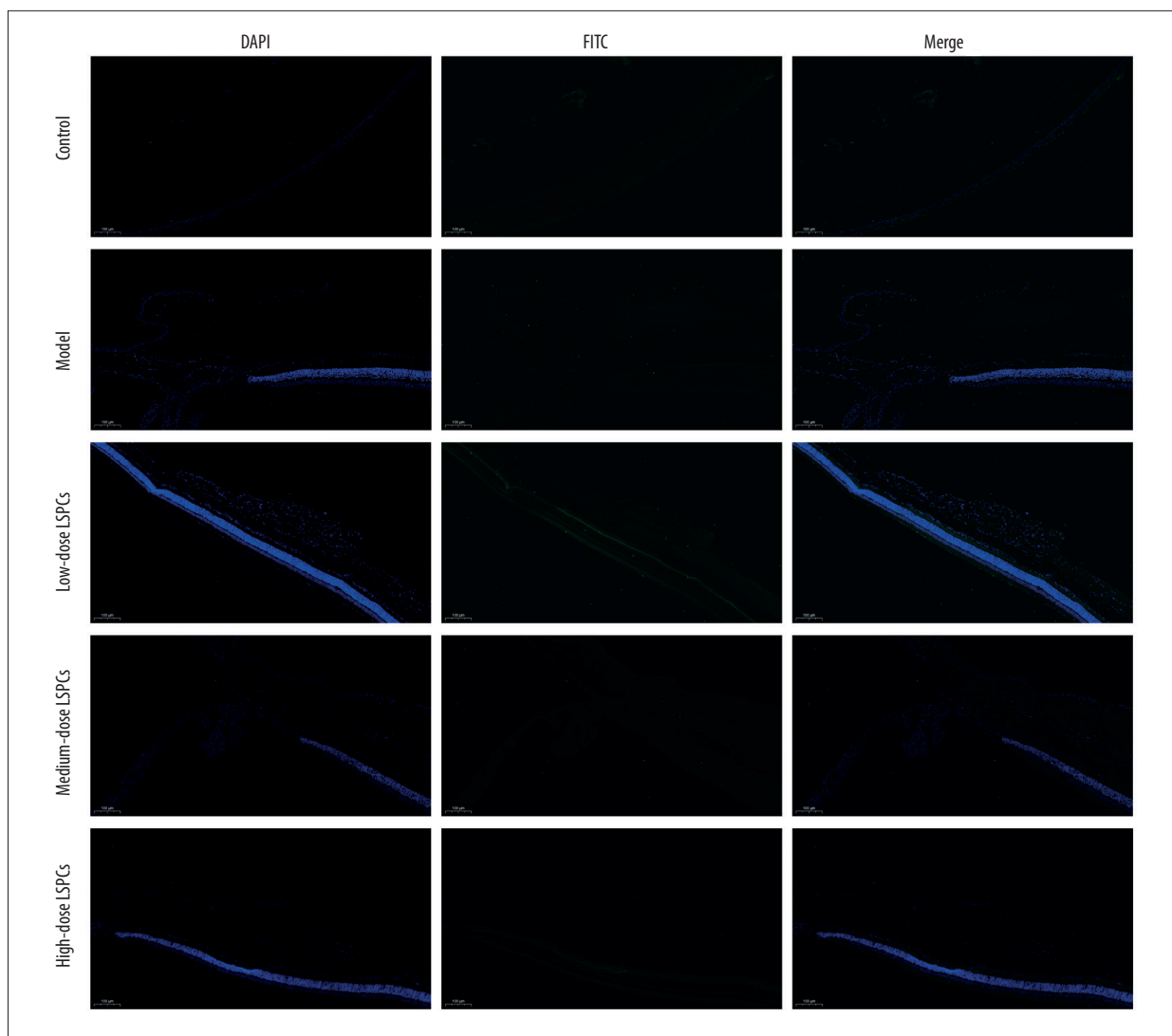


**Figure 5.** Treatment of LSPCs ameliorated light-induced cell apoptosis in vivo. TUNEL-positive cells were labeled in retinal sections. Representative photos of TUNEL staining of retinal sections from control, light-induced retinal damage model, low-, medium-, and high-dose LSPCs groups were shown, separately. Magnification, 100 $\times$ . Bar value, 100  $\mu$ m. Olympus software (version 2.2; Olympus, Japan) was used to create the pictures.

This indicated that LSPCs had neuroprotective effects in light exposure-induced retinal injury.

## Discussion

In this study, LSPCs effectively ameliorated light-induced retinal damage through the repeated instillation of LSPCs before the irradiation. Furthermore, LSPCs substantially suppressed the formation of oxidative stress-related markers and exerted anti-apoptosis and neuroprotective effects in the retina. Although previous studies have demonstrated that LSPCs possess potent antioxidant ability and protective effects on human health [12], this study shows for the first time that LSPCs have

physiologically and morphologically protective effects against light-induced retinal damage.

Retinal tissues are susceptible to oxidative stress due to their unique fatty acid composition and high oxygen consumption [16]. Oxidative stress participates in AMD, which is a major risk factor for visual loss as aging progresses [17]. Lipid peroxidation products like MDA, NO, and NOS can attack protein, DNA, and phospholipid, causing abnormal function of the retinal pigment epithelium and injury of photoreceptor cells [18]. Evidence suggests that dietary therapy with antioxidants can delay AMD development [19]. Oxidative stress is the major cause of neurodegeneration, which exerts critical roles in retinal degenerative disease [20]. In the present study, the



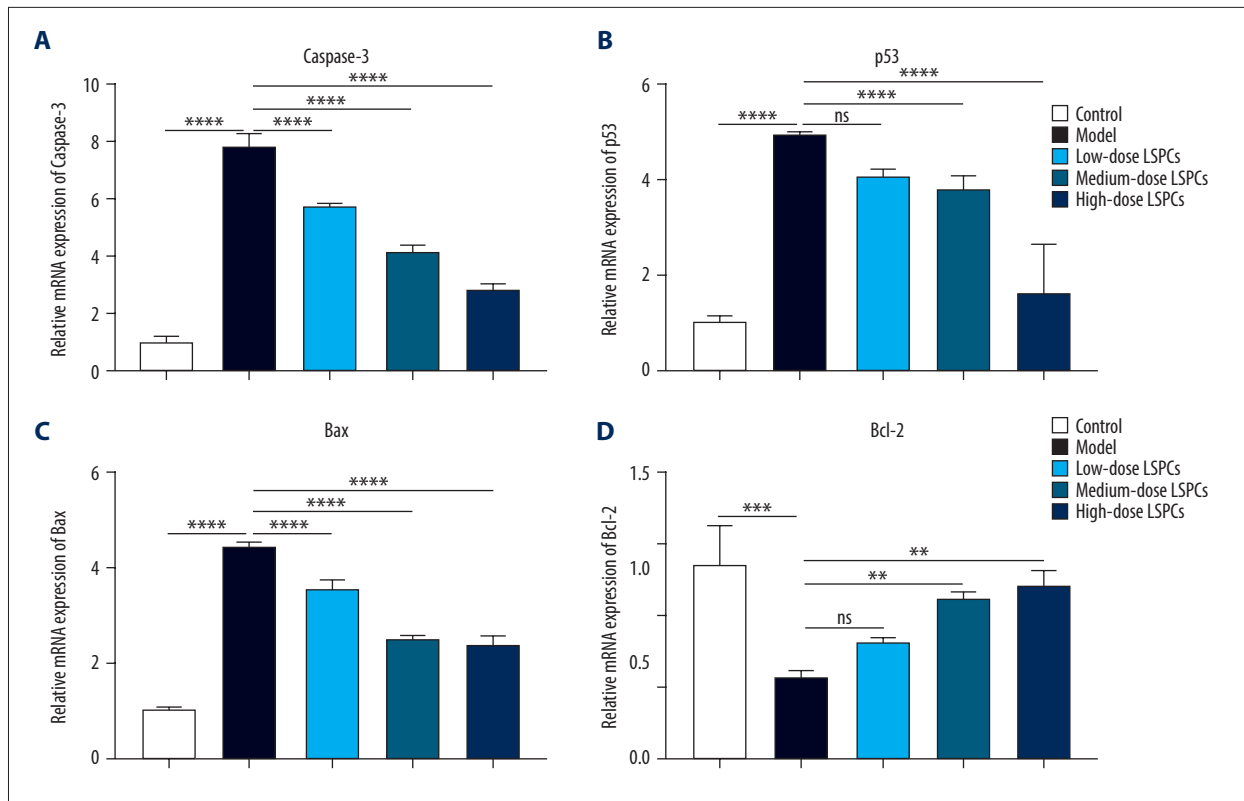


**Figure 6.** Treatment of LSPCs exerted an anti-apoptosis effect in light exposure-induced retina. (A-D) RT-qPCR was utilized for examining the expression of Caspase-3, p53, Bax and Bcl-2 mRNAs in retina from control, light-induced retinal damage model, low-, medium-, and high-dose LSPCs groups. Ns – not significant; \*\*  $P < 0.01$ ; \*\*\*  $P < 0.001$ ; \*\*\*\*  $P < 0.0001$ . GraphPad Prism software (version 8.0.1; Graph Pad; San Diego, CA, USA) was used to create the pictures.

light-induced retinal damage model rats displayed increased serum levels of the oxidative stress-relevant biomarkers MDA, NO, and NOS, as well as reduced activity of the antioxidant enzymes GSH-Px and SOD in comparison to controls, suggesting that oxidative stress participates in excessive light exposure-induced retinal damage.

Increasing evidence has strongly suggests that excessive light exposure mainly induces the apoptosis of photoreceptors and retinal ganglion cells [21]. In the present study, we observed the marked increase in the number of TUNEL-positive cells in the light-induced retinal damage model rats compared with controls. Treatment of LSPCs substantially reduced the number of TUNEL-positive cells in the light-induced retinal damage model rats in a dose-independent manner. Moreover, the light exposure-induced retinal injury model rats exhibited increased expression of apoptotic markers, including caspase-3, p53, and Bax, as well as the reduced expression of pro-apoptotic marker Bcl-2 in comparison to controls. In contrast, LSPCs markedly lowered the expression of the apoptotic markers caspase-3, p53, and Bax, and elevated the expression of pro-apoptotic marker Bcl-2 in the light exposure-induced retinal injury model rats. The expression of these proteins is primarily

modulated through genes and may reflect the alterations of gene functions. Hence, treatment with LSPCs may alleviate excessive light exposure-induced retinal apoptosis.

Müller cells are the main glial component in the sensory retinal tissue [22]. They exert critical roles in maintaining the homeostasis and metabolism of retinal neurons. Retinal neurons are more vulnerable to blue light, a major ingredient of visible light, compared with glial cells because of NA double-strand breaks [23]. Müller cells actively participate in almost all forms of retinal damage as well as other related diseases [24]. For instance, RS9, an activator of Nrf2, reduces light exposure-induced death of photoreceptor cells and Müller cells [25]. For response to injury, the reactive alterations of Müller cells are part of the process of gliosis, which can play a neuroprotective effect in the early stage following injury [26]. It has been reported that  $TNF\alpha$  can induce Müller cells to transform from non-proliferative gliosis to the retinal regeneration responses [27]. However, when Müller cells are overactivated, the overactive gliosis is harmful, forming glial scars and promoting retinal remodeling [28]. Retinal microglia may affect the behaviors of Müller cells induced by laser exposure [29]. The most sensitive non-specific response to gliosis is GFAP activation in the

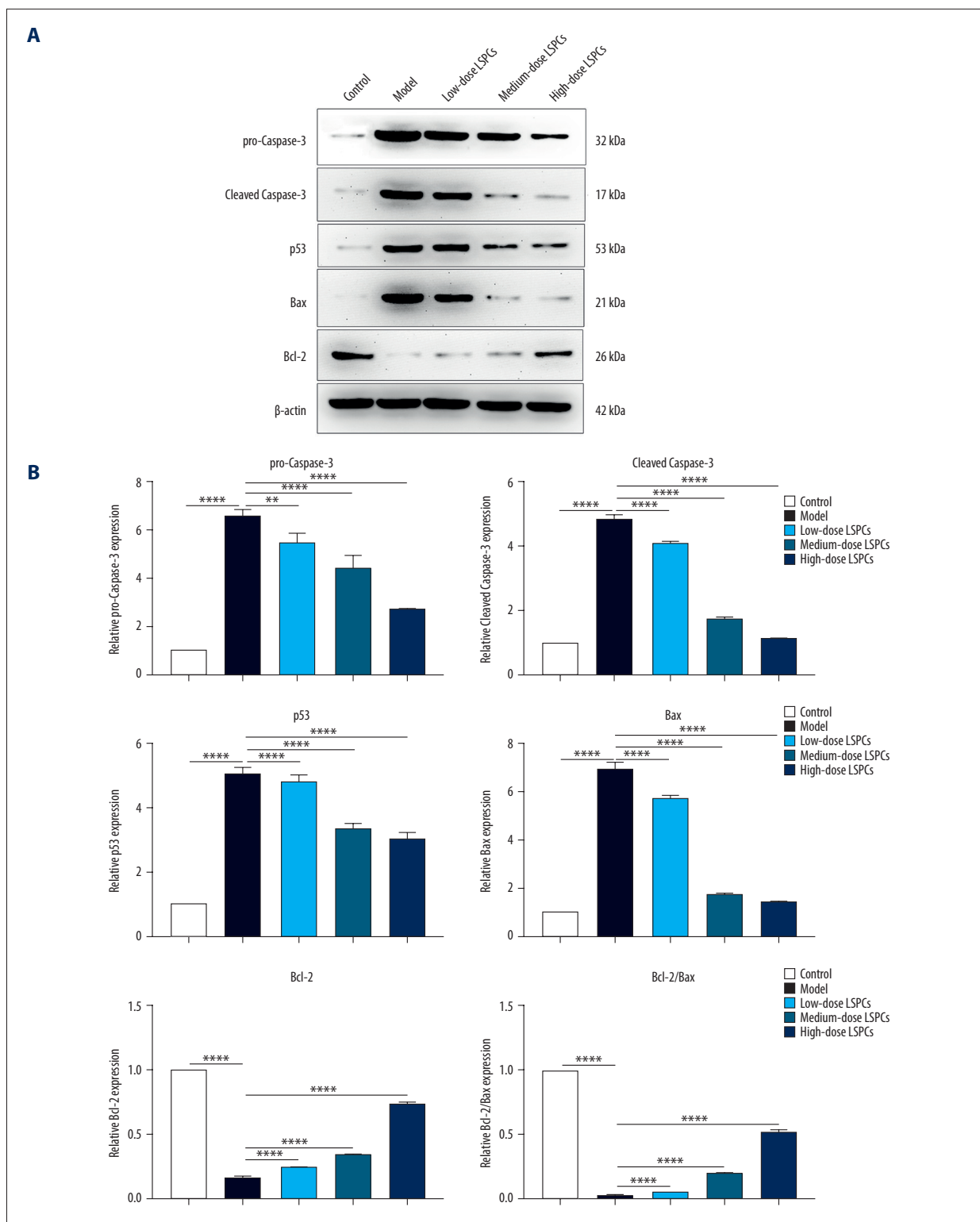


**Figure 7.** Treatment of LSPCs alleviated light exposure-induced cell apoptosis in retina. **(A)** Representative photos of western blotting for pro-Caspase-3, cleaved Caspase-3, p53, Bax as well as Bcl-2 proteins. **(B)** Quantification of the expressions of pro-Caspase-3, cleaved Caspase-3, p53, Bax, and Bcl-2 as well as Bcl-2/Bax ratio in retina from control, light-induced retinal damage model, low-, medium-, and high-dose LSPCs groups. \*\*  $P < 0.01$ ; \*\*\*\*  $P < 0.0001$ . GraphPad Prism software (version 8.0.1; Graph Pad; San Diego, CA, USA) was used to create the pictures.

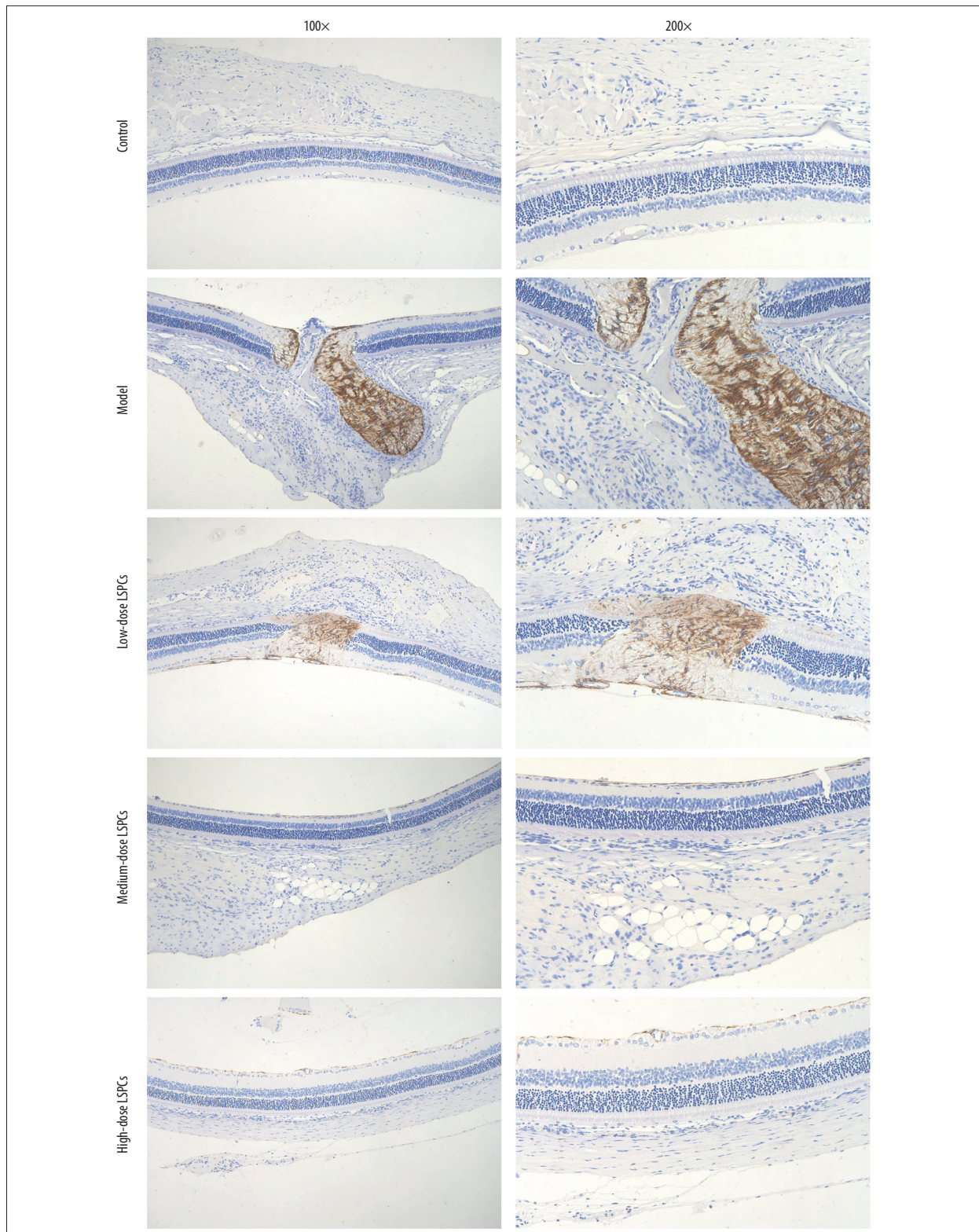


**Figure 8.** LSPCs exerted neuroprotective effects in light exposure-induced retina. IHC was carried out to examine the expression of GFAP protein in retinal tissues. Representative photos of IHC assay of retinal sections for control, light-induced retinal damage model, low-, medium-, and high-dose LSPCs groups are separately shown. Magnification, 100× or 200× bar value, 50 or 100 μm. Olympus software (version 2.2; Olympus, Japan) was used to create the pictures.



intermediate filament, which can be utilized as an indicator of Müller cell activation [30]. There is evidence that inhibiting the expression of GFAP has neuroprotective effects [31-33]. LSPCs ameliorate methyl-mercuric chloride damage-mediated neurotoxicity in neuron and astrocyte cells by modulating the activation of Nrf2/HO-1 as well as inhibiting the mitochondria-mediated apoptotic pathway [12]. In this study, the light-induced retinal model had higher GFAP expression than controls. LSPCs weakened light-induced GFAP activation in the retinal tissues in a dose-independent manner, indicative of the neuroprotective effects of LSPCs on light-induced retinal damage. However, in vivo models alone are not sufficient to validate the protective effect of LSPCs on retinal injury. More studies, including clinical trials, should be conducted to further confirm the therapeutic effects of LSPCs, which could offer novel insights into developing the clinical application of LSPCs.

## References:

- Zhao Y, Shen Y. Light-induced retinal ganglion cell damage and the relevant mechanisms. *Cell Mol Neurobiol.* 2020;40:1243-52
- Matsuo M, Kuse Y, Takahashi K, et al. Carteolol hydrochloride reduces visible light-induced retinal damage in vivo and BSO/glutamate-induced oxidative stress in vitro. *J Pharmacol Sci.* 2019;139:84-90
- Alejo-Armijo A, Salido S, Altarejos JN. Synthesis of A-type proanthocyanidins and their analogues: A comprehensive review. *J Agric Food Chem.* 2020;68:8104-18
- Zeng YX, Wang S, Wei L, et al. Proanthocyanidins: Components, pharmacokinetics and biomedical properties. *Am J Chin Med.* 2020;48:813-69
- Wang Y, de B Harrington P, Chang T, et al. Analysis of cranberry proanthocyanidins using UPLC-ion mobility-high-resolution mass spectrometry. *Anal Bioanal Chem.* 2020;412:3653-62
- Wei J, Yang J, Jiang W, Pang Y. Stacking triple genes increased proanthocyanidins level in *Arabidopsis thaliana*. *PLoS One.* 2020;15:e0234799
- Yang L, Xian D, Xiong X, et al. Proanthocyanidins against oxidative stress: From molecular mechanisms to clinical applications. *Biomed Res Int.* 2018;2018:8584136
- Nawrot-Hadzik I, Matkowski A, Hadzik J, et al. Proanthocyanidins and Flavan-3-ols in the prevention and treatment of periodontitis-antibacterial effects. *Nutrients.* 2021;13:165
- Tang R, Xian D, Xu J, et al. Proanthocyanidins as a potential novel way for the treatment of hemangioma. *Biomed Res Int.* 2021;2021:5695378
- Chen Y, Zhang R, Xie B, et al. Lotus seedpod proanthocyanidin-whey protein complexes: Impact on physical and chemical stability of  $\beta$ -carotene nanoemulsions. *Food Res Int.* 2020;127:108738
- Chen Y, Huang F, Xie B, et al. Fabrication and characterization of whey protein isolates- lotus seedpod proanthocyanin conjugate: Its potential application in oxidizable emulsions. *Food Chem.* 2021; 346:128680
- Zhang J, Zhang X, Wen C, et al. Lotus seedpod proanthocyanidins protect against neurotoxicity after methyl-mercuric chloride injury. *Ecotoxicol Environ Saf.* 2019;183:109560
- Gong YS, Guo J, Hu K, et al. Ameliorative effect of lotus seedpod proanthocyanidins on cognitive impairment and brain aging induced by D-galactose. *Exp Gerontol.* 2016;74:21-28
- Xiao J, Li S, Sui Y, et al. *Lactobacillus casei*-01 facilitates the ameliorative effects of proanthocyanidins extracted from lotus seedpod on learning and memory impairment in scopolamine-induced amnesia mice. *PLoS One.* 2014;9:e112773
- Xiao HB, Wang YS, Liang L, et al. Procyanidin B2 from lotus seedpod regulate NO/ADMA/DDAH pathway to treat insomnia in rats. *Fundam Clin Pharmacol.* 2019;33:549-57
- Anitua E, de la Fuente M, Del Olmo-Aguado S, et al. Plasma rich in growth factors reduces blue light-induced oxidative damage on retinal pigment epithelial cells and restores their homeostasis by modulating vascular endothelial growth factor and pigment epithelium-derived factor expression. *Clin Exp Ophthalmol.* 2020;48:830-38
- Koyama Y, Kaidzu S, Kim YC, et al. Suppression of light-induced retinal degeneration by quercetin via the AP-1 pathway in rats. *Antioxidants (Basel).* 2019;8:79
- Wang Y, Qi W, Huo Y, et al. Cyanidin-3-glucoside attenuates 4-hydroxynonenal- and visible light-induced retinal damage in vitro and in vivo. *Food Funct.* 2019;10:2871-80
- Zhang X, Henneman NF, Girardot PE, et al. Systemic treatment with nicotinamide riboside is protective in a mouse model of light-induced retinal degeneration. *Invest Ophthalmol Vis Sci.* 2020;61:47
- Li H, Liu B, Lian L, et al. High dose expression of heme oxygenase-1 induces retinal degeneration through ER stress-related DDIT3. *Mol Neurodegener.* 2021;16:16
- Dai M, Liu Y, Nie X, et al. Expression of RBMX in the light-induced damage of rat retina in vivo. *Cell Mol Neurobiol.* 2015;35:463-71
- Wang X, Liu Y, Ni Y, et al. Lentivirus vector-mediated knockdown of Sox9 shows neuroprotective effects on light damage in rat retinas. *Mol Vis.* 2019;25:703-13
- Chen P, Lai Z, Wu Y, et al. Retinal neuron is more sensitive to blue light-induced damage than glia cell due to DNA double-strand breaks. *Cells.* 2019;8:68
- Polosa A, Lv S, Ait Igrine W, Chevrolat LA, et al. Evidences suggesting that distinct immunological and cellular responses to light damage distinguishes juvenile and adult rat retinas. *Int J Mol Sci.* 2019;20:2744
- Inoue Y, Shimazawa M, Noda Y, et al. RS9, a novel Nrf2 activator, attenuates light-induced death of cells of photoreceptor cells and Müller glia cells. *J Neurochem.* 2017;141:750-65
- Albarracin R, Valter K. 670 nm red light preconditioning supports Müller cell function: Evidence from the white light-induced damage model in the rat retina. *Photochem Photobiol.* 2012;88:1418-27
- Iribarne M, Hyde DR, Masai I. TNF $\alpha$  induces Müller glia to transition from non-proliferative gliosis to a regenerative response in mutant zebrafish presenting chronic photoreceptor degeneration. *Front Cell Dev Biol.* 2019;7:296
- Osada H, Okamoto T, Kawashima H, et al. Neuroprotective effect of bilberry extract in a murine model of photo-stressed retina. *PLoS One.* 2017;12:e0178627
- Conedera FM, Pousa AMQ, Mercader N, et al. Retinal microglia signaling affects Müller cell behavior in the zebrafish following laser injury induction. *Glia.* 2019; 67:1150-66

## Conclusions

Collectively, this research provides the first evidence that LSPCs can alleviate retinal injury induced by light exposure. The potential mechanisms could involve antioxidative stress, anti-apoptosis, and neuroprotective mechanisms. Although in vivo experiments of our study support the beneficial effect of the novel therapeutic agent in alleviating light-induced retinal damage, in-depth human research is required to determine efficacy in clinical applications.

## Declaration of Figures' Authenticity

All figures submitted have been created by the authors, who confirm that the images are original with no duplication and have not been previously published in whole or in part.



30. Bahr HI, Abdelghany AA, Galhom RA, et al. Duloxetine protects against experimental diabetic retinopathy in mice through retinal GFAP downregulation and modulation of neurotrophic factors. *Exp Eye Res.* 2019;186:107742
31. Krishnan A, Kocab AJ, Zacks DN, et al. A small peptide antagonist of the Fas receptor inhibits neuroinflammation and prevents axon degeneration and retinal ganglion cell death in an inducible mouse model of glaucoma. *J Neuroinflammation.* 2019;16:184
32. Ueda H, Halder SK, Matsunaga H, et al. Neuroprotective impact of prothymosin alpha-derived hexapeptide against retinal ischemia-reperfusion. *Neuroscience.* 2016;318:206-18
33. Chen X, Amorim JA, Moustafa GA, et al. Neuroprotective effects and mechanisms of action of nicotinamide mononucleotide (NMN) in a photoreceptor degenerative model of retinal detachment. *Aging (Albany NY).* 2020;12:24504-21